

Water vapor condensation on binary mixed substrates: A molecular dynamics study

Zi-Jie Wang^{a,b}, Shao-Yu Wang^{a,b}, Dan-Qi Wang^{a,b}, Yan-Ru Yang^{a,b}, Xiao-Dong Wang^{a,b,*}, Duu-Jong Lee^{c,d,**}

^a State Key Laboratory of Alternate Electrical Power System with Renewable Energy Sources, North China Electric Power University, Beijing 102206, China

^b Research Center of Engineering Thermophysics, North China Electric Power University, Beijing 102206, China

^c Department of Chemical Engineering, National Taiwan University, Taipei 106, Taiwan

^d Department of Mechanical Engineering, City University of Hong Kong, Kowloon Tong, Hong Kong



ARTICLE INFO

Article history:

Received 19 August 2021

Revised 29 October 2021

Accepted 17 November 2021

Available online 28 November 2021

Keywords:

Condensation

Hybrid wetting substrates

Molecular dynamics simulation

Binary mixed substrates

ABSTRACT

Sophisticated and expensive surface texture design and manufacturing are commonly needed to achieve efficient surfaces with enhanced condensation performances. The high nucleation rate and high droplet removal capacity of a substrate surface acquire trade-off, whose mechanisms have not explicitly been comprehended. Based on the assumption that hydrophilic spots would improve nucleation while a hydrophobic surface can facilitate droplet removal rate, this work studied the nucleation and departure processes on a binary mixed substrate with randomly distributed hydrophilic atoms, with homogeneous substrates being as comparison references. The molecular dynamics simulation results showed that the wettability of the binary mixed substrate could be estimated by the form of the Cassie equation. Unlike the randomly nucleated clusters on a homogeneous substrate, the surface energy analysis verifies that the clusters tend to form on the areas with enriched hydrophilic atoms on a binary mixed substrate. Conversely, the droplets also tend to stick on the hydrophilic areas to deteriorate droplet removal efficiency. Combined with a probability analysis by the Monte Carlo method and MD simulation, a moderated ratio ($r_m = 25\%$ in this work) was shown to furnish better nucleation properties with minimal deterioration in departure properties than the mono-wettability substrate with the same contact angle.

© 2021 Elsevier Ltd. All rights reserved.

1. Introduction

Condensation is a phase change heat transfer process that finds wide applications in water desalination [1] and harvesting [2], cooling [3], power plants [4], and others. Condensation is classified into two categories, filmwise and dropwise, depending on the wettability of the cold substrate. On a hydrophilic substrate, the strong molecular attractive interaction between vapor and substrate would result in a reduced nucleation energy barrier to generate numerous droplets for easy coalescence into liquid film with a hindered heat transfer rate. Schmidt et al. [5] first observed the presence of dropwise condensation with gravity-induced sweeping droplets renewing the condensation surface. Condensation on

a hydrophobic substrate would redound to heat transfer even at a high nucleation barrier. The robust droplet removal properties enable the occurrence of more nucleation sites on a hydrophobic substrate, yielding one order of magnitude higher heat transfer rate than via filmwise condensation [6].

The surface properties of the cold substrate have a vital influence on the way vapor condenses. Inspired by the water repellence effects by lotus leaves [7], various bionic-inspired nano/microstructured substrates were proposed to maintain a robust dropwise condensation. On a microtextured substrate, the Cassie state of the condensate is more preferred than the Wenzel state due to the robust departure properties for the former. Thus, a surface accommodating the reliable transition from the Wenzel to the Cassie state is desired for condensation applications. Condensate can first penetrate the structure and stay in the metastable Wenzel state, then transit to the Cassie state as the droplet further grows and coalesces [8]. Except for the wetting transition-induced droplet departure, the coalescence-induced self-propelled droplet with a critical diameter of 10 μm on a superhydrophobic surface was reported [9]. Compared with the gravity-induced departure of water, the departure size of the coalescence-induced

* Corresponding author at: State Key Laboratory of Alternate Electrical Power System with Renewable Energy Sources, North China Electric Power University, Beijing 102206, China.

** Corresponding author at: Department of Chemical Engineering, National Taiwan University, Taipei 106, Taiwan.

E-mail addresses: wangxd99@gmail.com (X.-D. Wang), djlee@ntu.edu.tw (D.-J. Lee).

jumping droplet is reduced by at least two orders of magnitude. Heat and mass transfer properties for macroscale droplets can be directly characterized with experiments: the coalescence-induced droplet departure on the simple fabricated silanized copper oxide surfaces can enhance the condensation coefficient in 30 and 25% higher heat flux than state-of-the-art hydrophobic condensing surfaces at low supersaturations [10]. Based on the single droplet heat transfer model and number density of droplets at different sizes, a heat transfer model was proposed considering the coalescence induced jumping droplets which proposed that with a specific range of geometry 190% overall surface heat flux enhancement over conventional flat condensing surfaces can be achieved [11].

Despite the superior condensation performance on structured hydrophobic substrates, the nucleation barrier is high and nucleation sites cannot be controlled. Especially when the vapor is at high supersaturation, the rapid nucleation accompanied by randomly distributed nucleation sites will result in uncontrollable flooding; thus, the superhydrophobic substrate may lose its advantages in promoting droplets' departure. Inspired by the water capture effects of desert beetle [12], hybrid wetting substrates have been designed to improve condensation efficiency. When condensation occurs on the hybrid wetting substrate, nucleation is facilitated by hydrophilic spots, and the droplet removal is promoted comparing with the mono-hydrophilic surface. Adding the hydrophilic areas can manipulate the local nucleation barrier and control the spatial distributions of nucleation sites. The texture hydrophobic surface with hydrophilic tops prefer Cassie state droplets have superior shedding properties to enhance condensation heat transfer rate [13]. Ölçeroğlu and McCarthy [14] combined an array of superhydrophilic islands with superhydrophobic surfaces, thus promoted the self-organization of macroscale droplets and delay flooding on these mixed wettability substrates. Furthermore, as supersaturations increase, the mode of departure transitions from jumping to shedding with no flooding phenomena observed. Combined the advantages of nucleation on a hydrophilic substrate and droplet departure from a hydrophobic substrate, a hybrid wetting substrate was created to manipulate the maximum droplet radius and droplet size distribution, so producing a 23% heat transfer rate higher than the complete dropwise condensation mode at 2° of surface subcooling [15]. Some engineered surfaces, like SLIPPERY surfaces [16,17], are also proposed to balance the counter effects between maximum droplet radius and droplet size distribution on condensation heat transfer.

Nucleation is the first process of condensation, and it is crucial when improving the condensation efficiency. To the scale of nucleation, molecular dynamics (MD) simulation has been proven an efficient tool for mechanism exploration [18,19]. The nucleation rate and critical cluster size obtained from MD simulation agree with those from classical nucleation theory [20]. The condensation types, filmwise or dropwise, were also studied in nanoscale processes. Pu et al. [21] investigated the influence of wettability and subcooling on condensation mode. The results indicated that the condensate film would contract and rupture to droplets when reducing the substrate's wettability and would continue growing promoted by higher subcooling. As condensation occurs on a structured surface, the wetting transition and coalescence-induced jumping droplet would lead to efficient removal properties as with macroscopic surfaces. Gao et al. [22] reveal that the Cassie state droplets appeared on a textured surface with a high solid surface fraction, and would gradually transit from Cassie to Wenzel state as the fraction of the solid surface continuously decreased. The spatial control of nucleation was also studied by MD simulation. For vapor condensation on the plane surface with hydrophilic spots, the condensate would first be trapped on the spot, then the droplet growth in a near-constant contact line, and finally reaching to a state with a constant contact angle [23]. Gao et al. [24] studied

the condensation on hybrid nanopillar surfaces. Their results indicated that the hybrid nanopillars could manipulate the occurrence of nucleation and subsequent droplet growth. Although with studies abovementioned, special structural designs are needed for enhanced condensation performance on the substrate. Also, the relationship between the wettability with the added hydrophilic areas is unclear. More recently, Xing et al. [25] reported a cost-effective substrate with spraying the microdrop which contains PVA particle(hydrophilic) on a superhydrophobic surface and the randomly distributed hydrophilic region could markedly enhance condensation heat and mass transfer(240% average microdrop density with 387% self-removal rate comparing with superhydrophobic surface). Thus, the mechanisms of nucleation on a hybrid wetting substrate without state-of-the-art textures warrant further investigation.

In this article, the nucleation of water vapor and departure of water nanodroplet on the plane, binary mixed surfaces were studied via MD simulation. Inspire by the disordered alloy substrate [26], binary mixed substrates with randomly distributed hydrophilic atoms were designed. These binary mixed substrates may be produced by dissolving when the high-temperature alloy droplet is wetting on the substrates [27] or spraying hydrophilic particles on a hydrophobic substrate. The motivation of this work is to show that the substrate without state-of-the-art manufacturing textures can also provide enhanced condensation from a molecular perspective. The present results indicate that the binary mixed substrate with a moderated hydrophilic atomic ratio can furnish better nucleation properties and no obvious deterioration in departure properties than the mono-wettability substrate with the same contact angle.

2. Simulation method

Simulations of wetting and condensation were conducted using MD simulation. The construction of nanodroplets and vapor phase was performed using the packmol software. The simplified Au-like FCC substrates with different interactions were used to represent substrates with varying wettability. The schematic diagrams of the simulations are shown in Fig. 1. For the wetting system, a nanodroplet consisting of eight thousand molecules was placed on the substrate. The initial diameter of the nanodroplets was set as 7.5 nm. The substrate with height $H = 10.2 \text{ \AA}$, width $W = 200 \text{ \AA}$, and length $L = 200 \text{ \AA}$ was employed. The contact angle was measured when the spreading process reached equilibrium. As for the condensation system, water vapor consisting of one thousand molecules was distributed evenly in the simulation box. The size of the substrate was kept the same as in the wetting system. Two types of atoms were randomly mixed with different hydrophilic atomic ratios for the binary mixed substrate. When preparing the binary mixed substrates, The Mersence Twister (MT19937) was used to decide the type of the atom at each FCC point according to the hydrophilic atomic ratios [26,28].

The MD simulations were performed using the large-scale atomic/molecular massively parallel simulator package [29]. The embedded-atom method was used for describing the interatomic forces of Au-like atoms [30]. The SPC/E water model was employed for calculating the interactions between water molecules [31]. The 12–6 Lennard-Jones and Coulombic potentials were employed to describe the interactions between Au-like substrate and water molecules [32]:

$$U_{ij} = 4\epsilon_{ij} \left[\left(\frac{\sigma_{ij}}{r_{ij}} \right)^{12} - \left(\frac{\sigma_{ij}}{r_{ij}} \right)^6 \right] + \frac{q_i q_j}{r_{ij}} \quad (1)$$

where ϵ represents the depth of the potential well, σ is the distance where the inter-particle potential is zero, q_i and q_j are the electric charges of atom i and j , respectively. r_{ij} is the distance be-

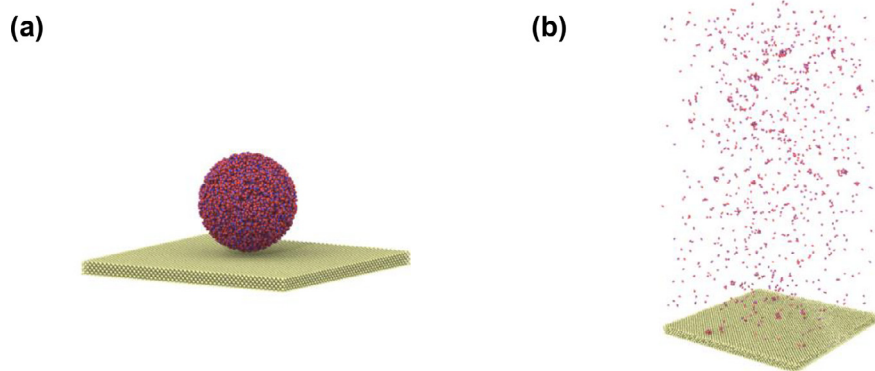


Fig. 1. Schematic diagram for simulation systems: (a) wetting system and (b) condensation system.

Table 1

Potential energy parameters among particles in the simulation.

Particles i, j	q (e)	σ_{ij} (\AA)	ε_{ij} (eV)
H-H	+0.4238	0.000	0.0000
O-O	-0.8476	3.166	0.0067
H-Au		0.0000	0.0000
O-Au		2.8675	0.006–0.015

tween atom i and atom j . The cutoff distance of 10 \AA was used for the 12-6 LJ potential. The simulation parameters were listed in Table 1. The changing energy parameter ε leads to a different interaction between water molecules and substrate.

The whole system used the NVT ensemble with 293 K for the wetting simulations until the droplet reached equilibrium. For the condensation simulation, the entire system was equilibrated at 373 K with the NVT ensemble until the system was kept at a minimum energy level. Then the temperature of the substrate was decreased to 293 K for another simulation for 7 ns to observe the occurrence of nucleation. The Velocity-Verlet algorithm [33] was applied to describe the motions of individual atom at a time-step of 1 fs. Periodic boundary conditions were applied along the x -and the y -direction, and the non-periodic fixed condition with reflex boundary was applied to the top of the simulation box. For the latter, in case a water molecule touched the top boundary, it would be bound back without losing energy.

The cluster analysis program was written using the C++ programming language. A molecule whether in a cluster was identified inspired by the Stillinger criterion [34]. The threshold distance between two oxygen atoms was 3.36 \AA in one cluster [23]. And whether a cluster was on the surface was determined using the same distance. The visualization of the simulation was using OVITO software [35].

3. Results and discussion

3.1. Wettability of binary mixed substrates

The substrate wettability significantly affects the type of condensation, dropwise and filmwise in particular. The Young's equation was used to quantify the wettability of an ideal plane surface by contact angle [36]:

$$\sigma_{lv} \cos \theta = \sigma_{sv} - \sigma_{sl} \quad (2)$$

where σ_{lv} , σ_{sv} , and σ_{sl} are the liquid-vapor, solid-vapor, and solid-liquid interfacial tension, respectively. In MD simulation, interaction parameters were used to characterize the energy of substrates. Due to the thermal fluctuation appeared at the vapor-liquid interface, a statistical method was adopted to characterize the contact

Table 2

Calculated contact angle(CA).

CASE	$\varepsilon_{0\text{-Au}}$ (eV)	CA($^\circ$)	Fitting error ($^\circ$)
1	0.006	139.9	0.96
2	0.00699	131.9	0.47
3	0.00825	122.6	0.36
4	0.010	108.3	0.79
5	0.01225	94.7	0.56
6	0.015	74.9	1.63

angle [37]: the last 50 timesteps were used to count the number density of the droplet at equilibrium shape (Fig. 2(a) and (c)). The boundary was then defined by half of the bulk water density [22], and the density profile along the centerline of the water droplet has shown in Fig. 2(b). The shell(marked in Fig. 2(c) with dash line) decided by the boundary(marked in Fig. 2(c) with the red circle) is used to calculate the contact angle. A circle fitting method was used to calculate the static contact angle (Fig. 2(d)), with the contact angle being measured by the slope of the fitted line at the droplet contact base. The fitting errors were calculated by the absolute errors of the location and radius of the fitted circles. The relationship between the contact angle and water-substrate interaction is listed in Table 2.

In this work, the hydrophilic atoms ratio r_m defines the percentage of hydrophilic atoms in the substrate: r_m of 0 and 1 represent mono-hydrophobic/hydrophilic substrate, respectively. The hydrophobic and hydrophilic atoms with energy potential $\varepsilon = 0.006$ and 0.015 are chosen for the testing mix. To study the influence of r_m on the wettability, nanodroplets were placed on substrates with $r_m = 11.11\%$, 25.00% , 44.46% , and 69.44% . The contact angle was decreased with increasing hydrophilic atom ratio. Specifically, a linear relationship between the cosine value of droplet contact angle and the r_m is found. It is indicated when a binary substrate is mixed by hydrophobic atoms and hydrophilic atoms, the apparent contact angle on the randomly mixed substrate θ_m can be estimated by the form of Cassie equation [38]:

$$\cos \theta_m = r_m \cos \theta_i + (1 - r_m) \cos \theta_o \quad (3)$$

where θ_o and θ_i are the intrinsic contact angles on the hydrophobic and hydrophilic substrates, respectively. The comparison between the predicted value from Eq. (3) and the result of MD simulation is shown in Fig. 2(e). This equation indicates that the introduced hydrophilic areas would increase the wettability of the hybrid wetting substrates, making it hard to distinguish the contribution of increased wettability or action of hydrophilic spots on the improved nucleation. Thus, the nucleation and departure process on the binary mixed substrate and the mono-wettability sub-

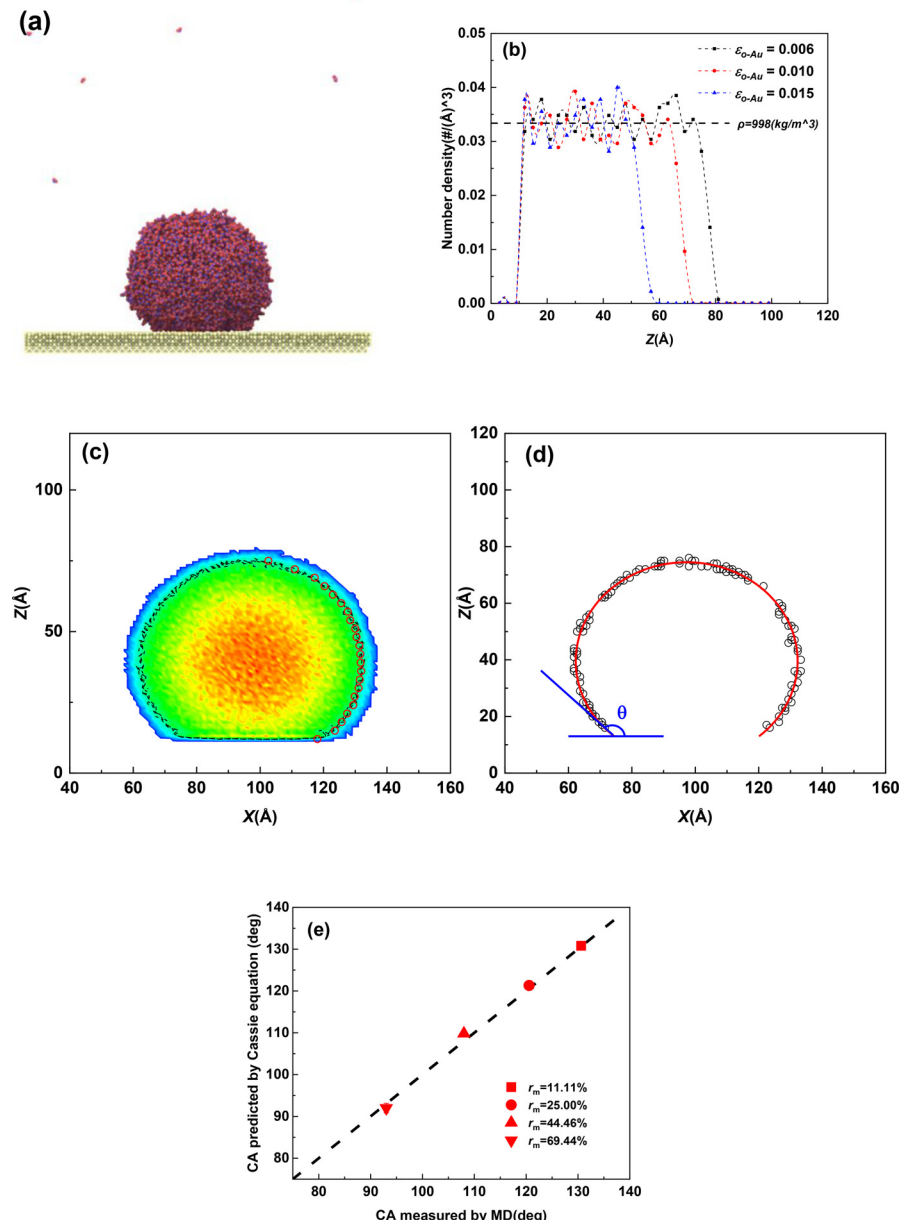


Fig. 2. Contact angle of water nanodroplet as a function of hydrophilic atom ratio. ((a) snapshot of the nanodroplet on the substrate, (b) number density profile along the centerline of the water droplet, (c) to (d) is the method to measure the contact angle, the contact angle on the binary mixed substrate can be estimated by the form of the Cassie equation and (e) shows the comparison between the predicted value and simulation result).

strate with the same wettability were discussed in the following section.

3.2. Nucleation on the binary mixed substrate

The nucleation process on hydrophobic, hydrophilic, and the mixed substrate with $r_m = 25\%$ were simulated. The nucleation simulation was also implemented on the mono-wettability substrate as a contrast, which has the same contact angle as the binary mixed substrate. From the classical nucleation theory (CNT) perspective, the nucleation energy barrier was derived from CNT to account for the difficulty of the nucleation process [20]:

$$\Delta G^* = \frac{16\pi \sigma_{lv}^3}{3\rho^2 \Delta\mu^2} F \quad (4)$$

where ρ is the density of the liquid, $\Delta\mu$ is the chemical potentials difference between the vapor and liquid phase, and the Fletcher

factor $F = [(2 - 3\cos\theta + \cos^3\theta)/4]$ is a geometry parameter representing different wetting states where θ is the equilibrium contact angle. In the nucleation energy barrier perspective, as the contact angle changes (ideally) from 0 to 180°, the Fletcher factor is increased from the minimum of zero to 4: the hydrophilic substrate has preferable nucleation properties since it has reduced energy barrier. Furthermore, the threshold cluster size was derived from the CNT to account for the stability of the cluster [20]:

$$n^* = \frac{32\pi \sigma_{lv}^3}{3\rho^2 (k_b T \ln S)^3} F \quad (5)$$

where k_b is Boltzmann constant and S is supersaturation ratio. The average thermal-hydraulic parameters based on current simulations were used to calculate the threshold cluster size. When vapor was nucleated on a hydrophobic substrate, the threshold cluster size was estimated to be 37 from CNT. But the threshold cluster

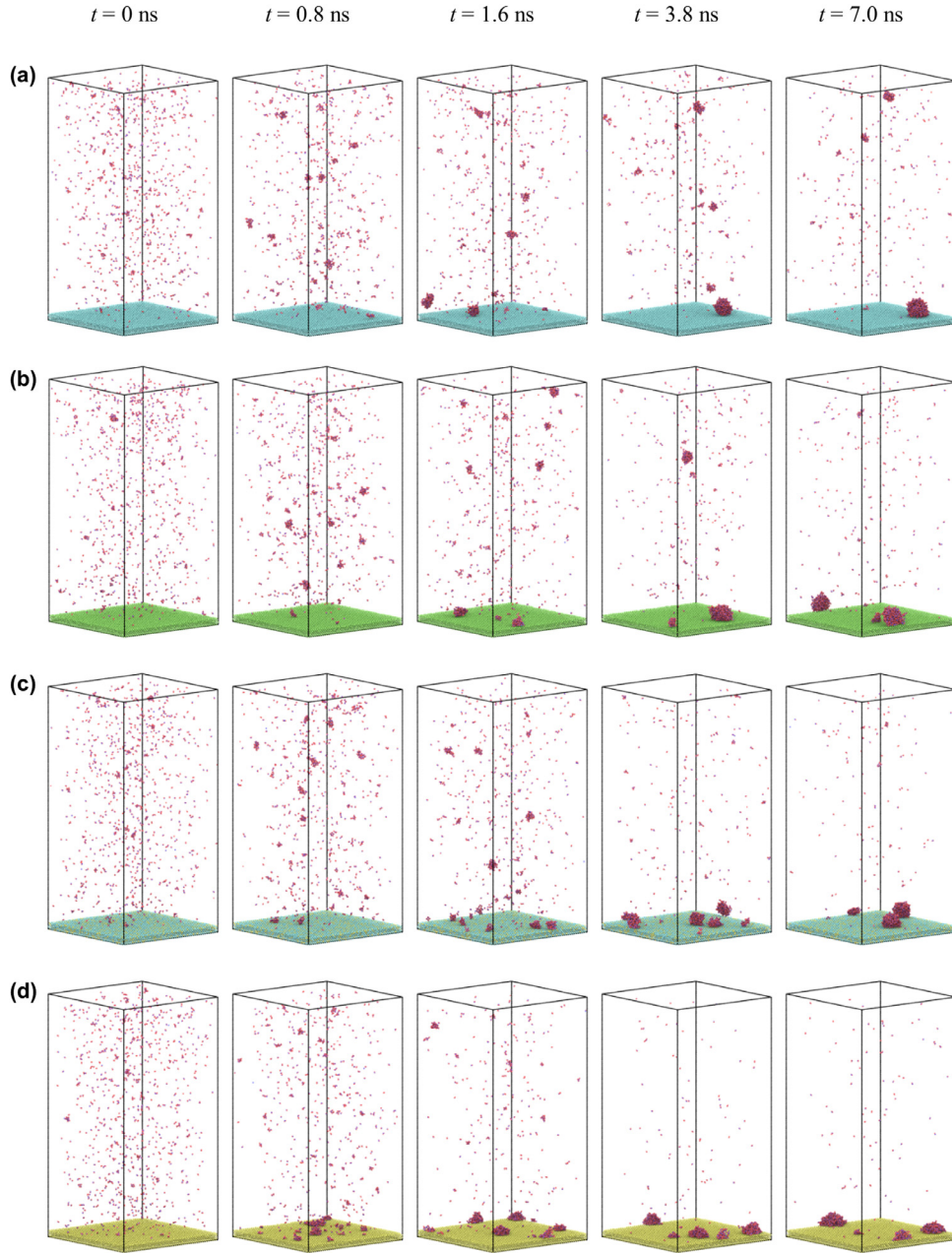


Fig. 3. Snapshots for vapor nucleation on (a) the hydrophobic substrate, (b) the contrast substrate, (c) the binary mixed substrate with $r_m = 25.00\%$, and (d) the hydrophilic substrate.

size was estimated to be 17 for hydrophilic case. It is easier for a cluster with a few water molecules exist on the hydrophilic substrate compare with the hydrophobic substrate. For the simualntion, the snapshots of the nucleation process are shown in Fig. 3. When the vapor is nucleated on the hydrophobic substrate, most of the clusters appear in the bulk phase. Partial clusters would also occur on the substrate, move around, and even bound back to the bulk phase. A similar bound-back phenomenon was also reported in Ref. [23]. Different from nucleation on a hydrophobic substrate, the preferable nucleation property of hydrophilic substrate is manifested by the repaid nucleation on the surface. The nucleation phenomenon on the contrast substrate is somehow between that on a hydrophobic and a hydrophilic substrate. Comparing with the contrast substrate, when nucleated on the binary mixed sub-

strate, a distinct increase in the number of clusters (Fig. 3(c) at 1.6 ns) indicates the boosting of nucleation on the binary mixed substrate.

For an insight into the kinetic behavior of the clusters during the nucleation process, the top view snapshots of the near-wall area ($z < 50 \text{ \AA}$) are selected, as shown in Fig. 4. When nucleated on the mono-wettability substrate, the water clusters are randomly distributed, correlating to the nature of the surface. When the vapor is nucleated on a hydrophobic substrate, weak substrate-water interaction hinders the nucleation process, making a distinct cluster occur at $t = 1.5 \text{ ns}$, which is postponed than that on a hydrophilic surface ($t = 0.8 \text{ ns}$). Moreover, the formed cluster is even movable on a hydrophobic substrate, as shown in Fig. 4(a). On a hydrophilic substrate, conversely, the strong solid-liquid interaction

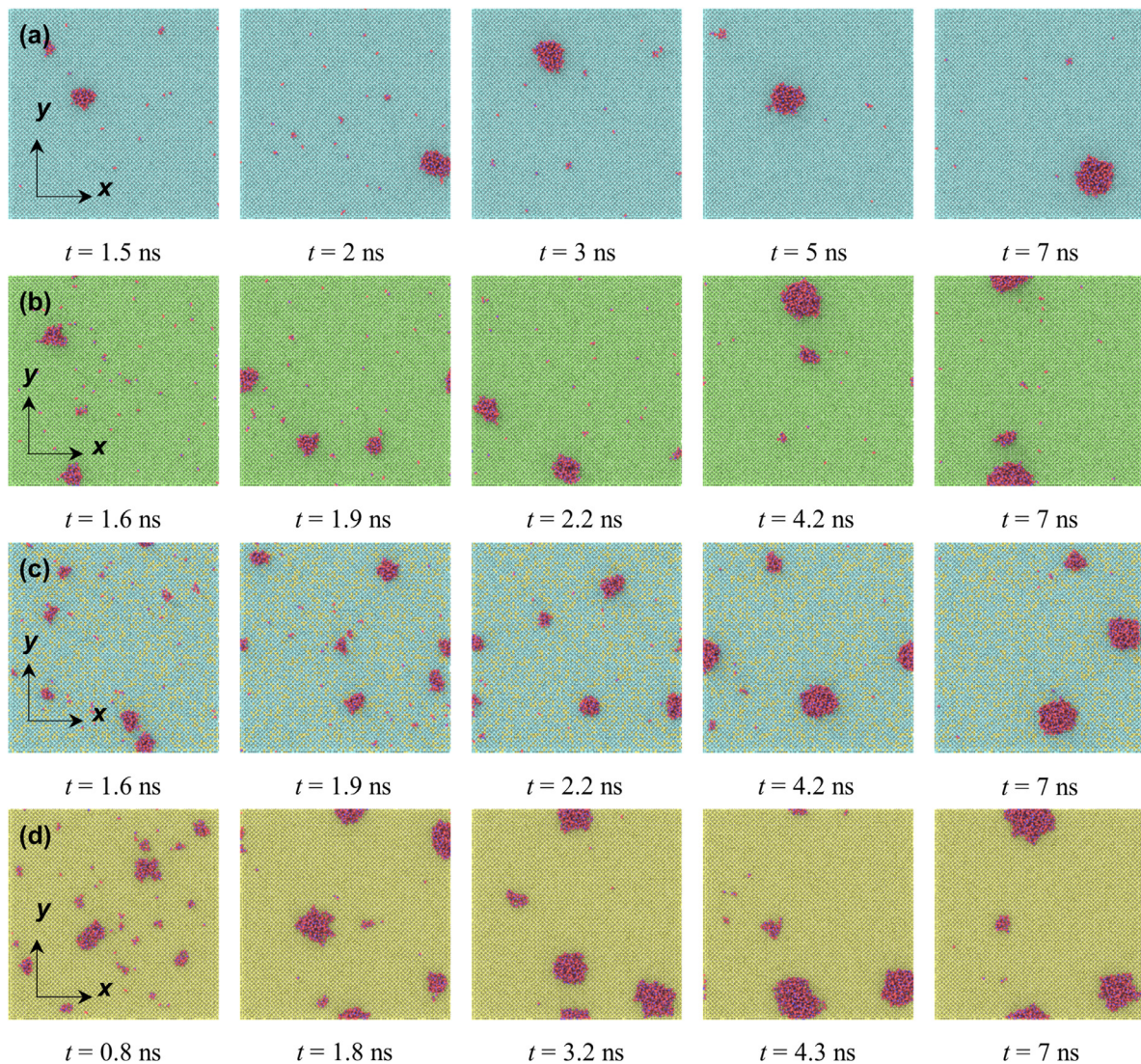


Fig. 4. Top view of the nucleation on (a) the hydrophobic substrate, (b) the contrast substrate, (c) the binary mixed substrate with $r_m = 25.00\%$, and (d) the hydrophilic substrate.

increases the number of nucleated clusters, and the formed clusters would prefer to stick on the substrate. For the binary mixed substrate, despite the same wettability with the contrast substrate, the number of condensed clusters markedly increased, with some clusters sticking on the substrate. As for the aforementioned bound-back phenomenon, a cluster with 64 water molecules was observed to bound back to the bulk phase, as shown in Fig. 5(a). Compared with the homogeneous surface with the same wettability, the local high potential energy spots would make the binary mixed substrate having low nucleation barrier. As shown in Fig. 5(b) and (c), a small cluster with 22 molecules on the high energy spots of the binary mixed substrate was not back to the bulk phase but a larger cluster with 46 molecules is shown unstable on the contrast substrate. Thus, the locally high energy spots of the binary mixed substrate can capture a smaller cluster than that on homogeneous substrate at the same wettability, which makes the binary mixed substrate capability to improve the nucleation performance.

To better understand the behavior of the clusters on the binary mixed substrate, the surface energy analysis [39] was implemented. As Fig. 6(a) shows, the warm color denotes the distribution of hydrophilic atoms, and a continuous warm color area in-

dicates the high local concentration of hydrophilic atoms. Compared with the cool color area, a warm color area can consider to be a nucleation site. A snapshot at the initial stage of the nucleation was chosen to map onto Fig. 6(a), as shown in Fig. 6(b), all locations of nucleated clusters are consistent with high hydrophilic atoms concentration areas. Without a sophisticated structural manipulation that acquires expensive efforts, the randomly distributed hydrophilic atoms could induce the local high energy spots on the binary mixed substrate that can improve the nucleation density. The cluster analysis was used to quantify the nucleation performance, as shown in Fig. 7. During the nucleation process, the number of clusters is increased first, and then, the number would decrease due to the coalescence between clusters. Thus, the peak of cluster number in Fig. 7(a) can be regarded as the number of active nucleation sites. The number of clusters formed on the hydrophilic substrate surface is four times higher than that on the hydrophobic substrate at the initial nucleation stage, showing robust nucleation performance on the hydrophilic substrate. When nucleated on the binary mixed substrate and the contrast substrate, the cluster number on the former is two times higher than that on the latter despite at the same wettability of the substrates. Despite without a sophisticated surface design,

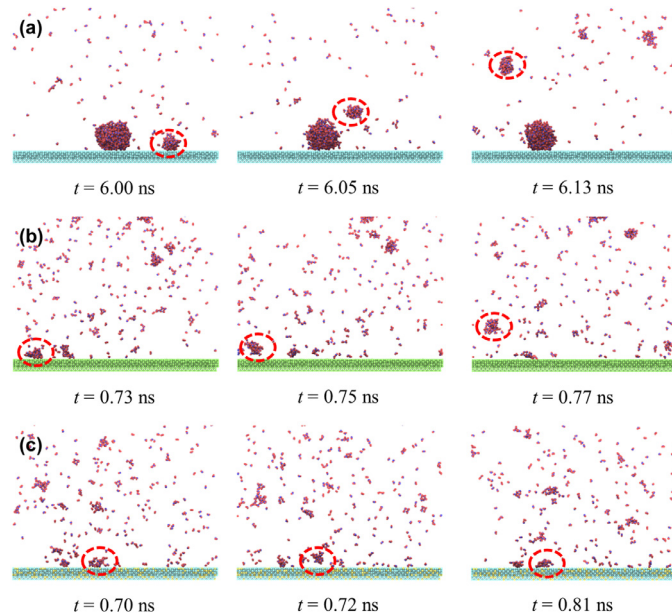


Fig. 5. The stability of the cluster on (a) the hydrophobic substrate, (b) the contrast substrate, and (c) the binary mixed substrate.

the randomly distributed hydrophilic atoms could induce locally high energy spots on the binary mixed substrate that can improve the nucleation performance. Fig. 7(b) shows the number of water molecules in the condensed clusters. For mono-wettability substrates, 710, 780, and 910 water molecules are condensed on the hydrophobic, contrast substrate and hydrophilic substrate, respectively. Restated, the condensed water molecules would increase with increasing wettability of the substrate. Compared with 780 water molecules condensed on the contrast substrate, 860 water molecules are condensed on the binary mixed substrate. Thus, the binary mixed substrate with randomly distributed hydrophilic atoms renders an avenue for increasing vapor nucleation performance.

3.3. Departure properties on the binary mixed substrate

A robust dropwise condensation benefited from the rapid cycle from nucleation to droplet departure. Thus, the departure properties also critically matter. For departure properties, gravity-induced droplet departure is depicted by the maximum departure radius [11,40]:

$$r_{\max} = \sqrt{\frac{3(\cos \theta_{\text{re}} - \cos \theta_{\text{ad}}) \sin \theta}{2F} \frac{\sigma_{\text{lv}}}{\rho g}} \quad (6)$$

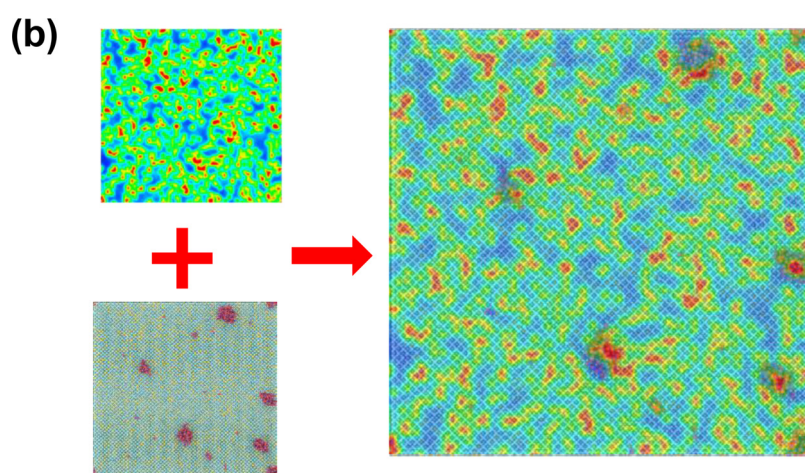
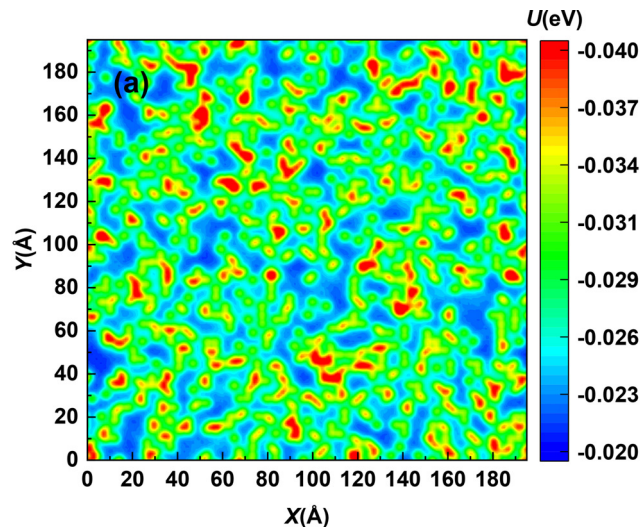


Fig. 6. (a) Potential energy between water molecule and the binary mixed substrate. (b) The location of the clusters consistent with the high potential energy distribution.

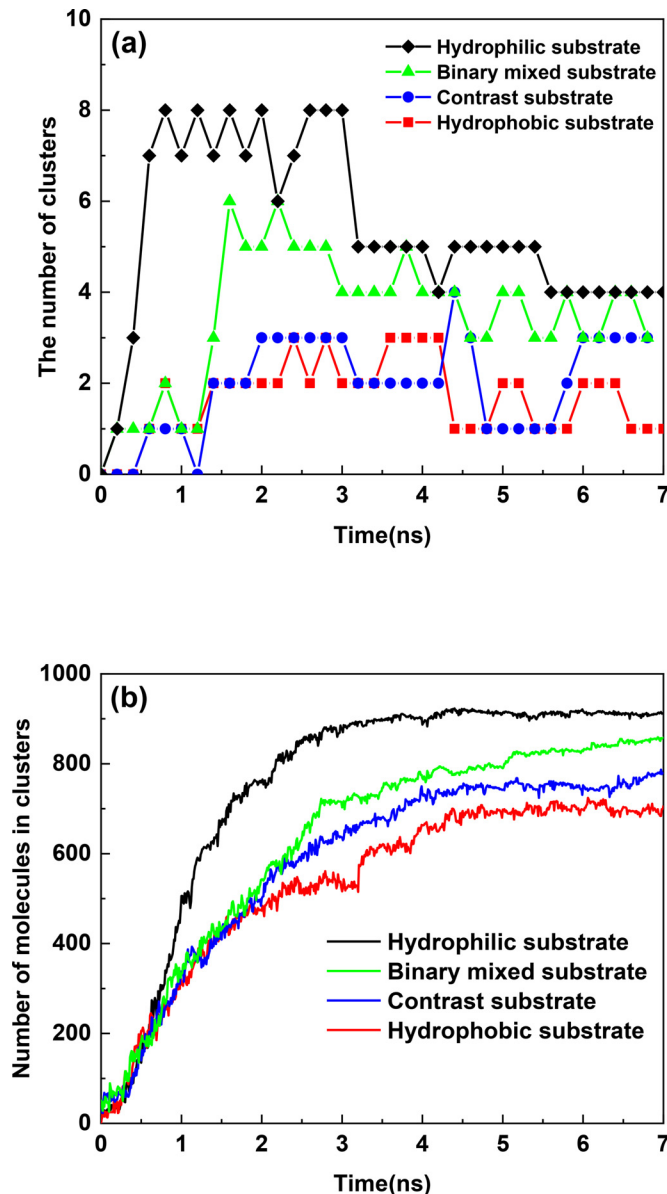


Fig. 7. (a) Number of clusters on the surface of substrates. (b) Evolution of the number of condensed vapor molecules on different substrates.

where θ_{re} and θ_{ad} are the receding and advancing contact angles, respectively; g is the gravity acceleration constant. The contact angle hysteresis (CAH) is defined by the difference between receding and advancing contact angles [41]. Thus, a large contact angle with a low contact angle hysteresis is demanded by the preferable departure properties.

In case to study the departure properties when the hydrophobic substrate mixed with hydrophilic atoms, a body force is exerted on the nanodroplet to mimic the driving force to counteract the resistance force of moving [42,43]. When the applied body force is larger than the resistance force of the moving contact line, the nanodroplet would move along the direction of the applied force. Although the homogeneous substrates in our study is smooth, the lattice vibrations of the substrate was one of the sources of the CAH. Thus, the CAH phenomenon can be find when nanodroplet slipping on the homogeneous hydrophilic substrate. The measure method of CAH for slipping nanodroplet is shown in Fig. 8. When the droplet slipping on a hydrophilic substrate, the CAH is large (27°) owing to the action of strong solid-liquid interaction force.

Table 3
The CAH of nanodroplet on different substrates.

CASE Group	Parameter	CA($^\circ$)	Fitting error ($^\circ$)	$\theta_{re}/\theta_{ad}(^\circ)$
1	$\varepsilon_{o-Au}=0.00699$ (H1) $r_m=11.11\%$	131.9	0.47	–
2	$\varepsilon_{o-Au}=0.00825$ (H2) $r_m=25.00\%$	122.5	0.36	118.4/124.3
3	$\varepsilon_{o-Au}=0.010$ (H3) $r_m=44.46\%$	108.3	0.79	97.4/109.3
4	$\varepsilon_{o-Au}=0.01225$ (H4) $r_m=69.44\%$	94.7	0.56	80.2/95.2
		92.0	1.14	82.5/100.1

Conversely, on a hydrophobic substrate, the relatively small CAH for the nanodroplet can be ignored, which was also reported in Ref. [43]. For the binary mixed substrate and the contrast substrate, their CAH's are similar (5.9° for the contrast substrate and 4.8° for the binary mixed substrate). The similar CAH on these different substrates can be interpreted by the molecular kinetic theory (MKT). The relationship between the advancing and receding contact angles based on the MKT can be written as [43]:

$$\cos \theta_{re} - \cos \theta_{ad} \sim \frac{R}{\gamma_v} \exp\left(\frac{E_0}{k_b T}\right) \quad (7)$$

where E_0 is the height of the energy barrier while R represents the droplet base radius. From Eq. (7), the energy barrier on the contrast substrate is higher than that on the hydrophobic substrate. The binary mixed substrate has 75% hydrophobic atoms; thus, although the binary mixed substrate has 25% hydrophilic atoms, the E_0 of the contrast substrate and the binary mixed substrate are similar. Thus, the CAH of the droplet is similar between the contrast substrate and the binary mixed substrate. With the same wettability and CAH, it can be deduced that the departure properties are similar for both the binary mixed substrate and the contrast substrate. This result indicates that the binary mixed substrate can improve the nucleation process of condensation with a small sacrifice on the departure performance. Thus, the binary mixed substrate with randomly distributed hydrophilic atoms has the ability to enhance condensation performance.

3.4. Effects of hydrophilic atom ratio on the vapor condensation

To explore the influence of hydrophilic atom ratio on the condensation performance on a binary mixed substrate, the ratio of 11.11%, 25.00%, 44.46%, and 69.44% were selected for further study. The mono-wettability substrates were also designed to make the comparison. The cases used in this section are listed in Table 3.

For the nucleation process, as shown in Fig. 9, when vapor molecules are nucleated on a binary mixed substrate with $r_m = 11.11\%$, the clusters are formed in a random manner. Besides, the clusters on the substrate are movable due to the low solid-liquid interaction force caused by the low hydrophilic ratio. With the ratio being increased to 25.00%, the enriched hydrophilic atoms in the substrate increase the number of local energy spots, generating more easily the condensed clusters on them. Then, the clusters would stick on the large high-energy spot, as shown with red dotted circles in Fig. 9(b). While increasing ratio, the increased hydrophilic atoms on the substrate surface would further increase the number of high energy spots, hence more clusters preferably form and stick on these spots. For vapor nucleated on a binary mixed substrate with 69.44% hydrophilic atoms, the increased hydrophilic ratio has led to enhance wettability, as expected, the nucleation rate was promoted.

To explore the nucleation processes quantitatively, the number of water molecules in the clusters was calculated as shown in Fig. 10. When the ratio is 11.11%, the number of condensed water molecules same as in the homogeneous substrate with the same

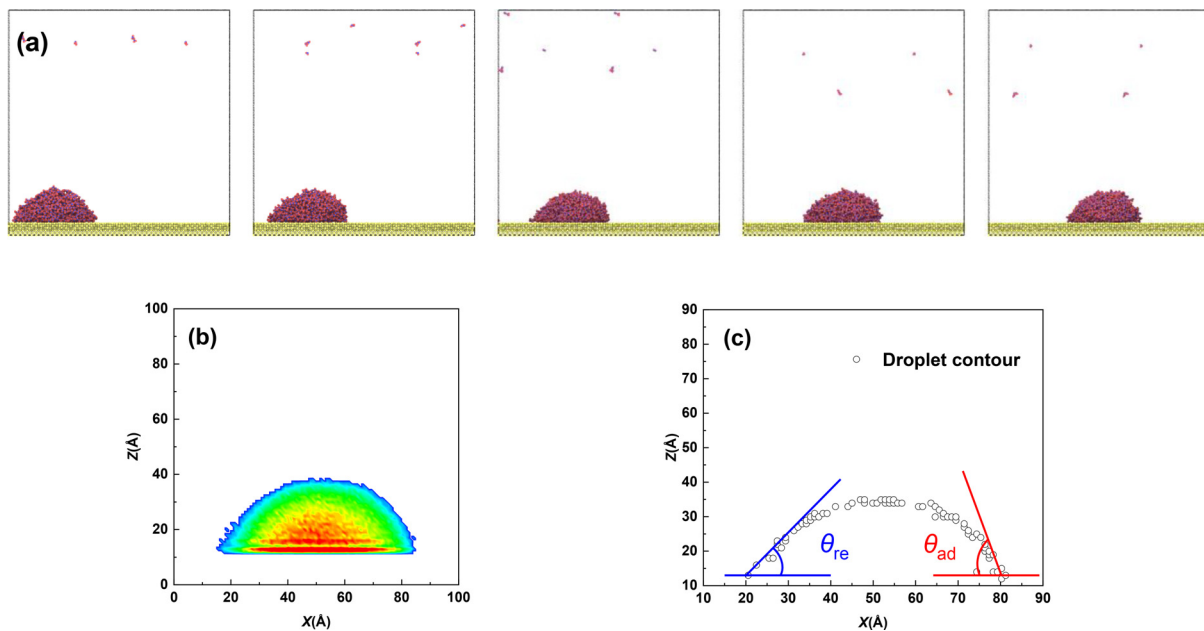


Fig. 8. (a) The slipping nanodroplet on the hydrophilic substrate. The CAH measure method: (b) number density of the droplet on the hydrophilic substrate and (c) measurement of the receding and advancing contact angle.

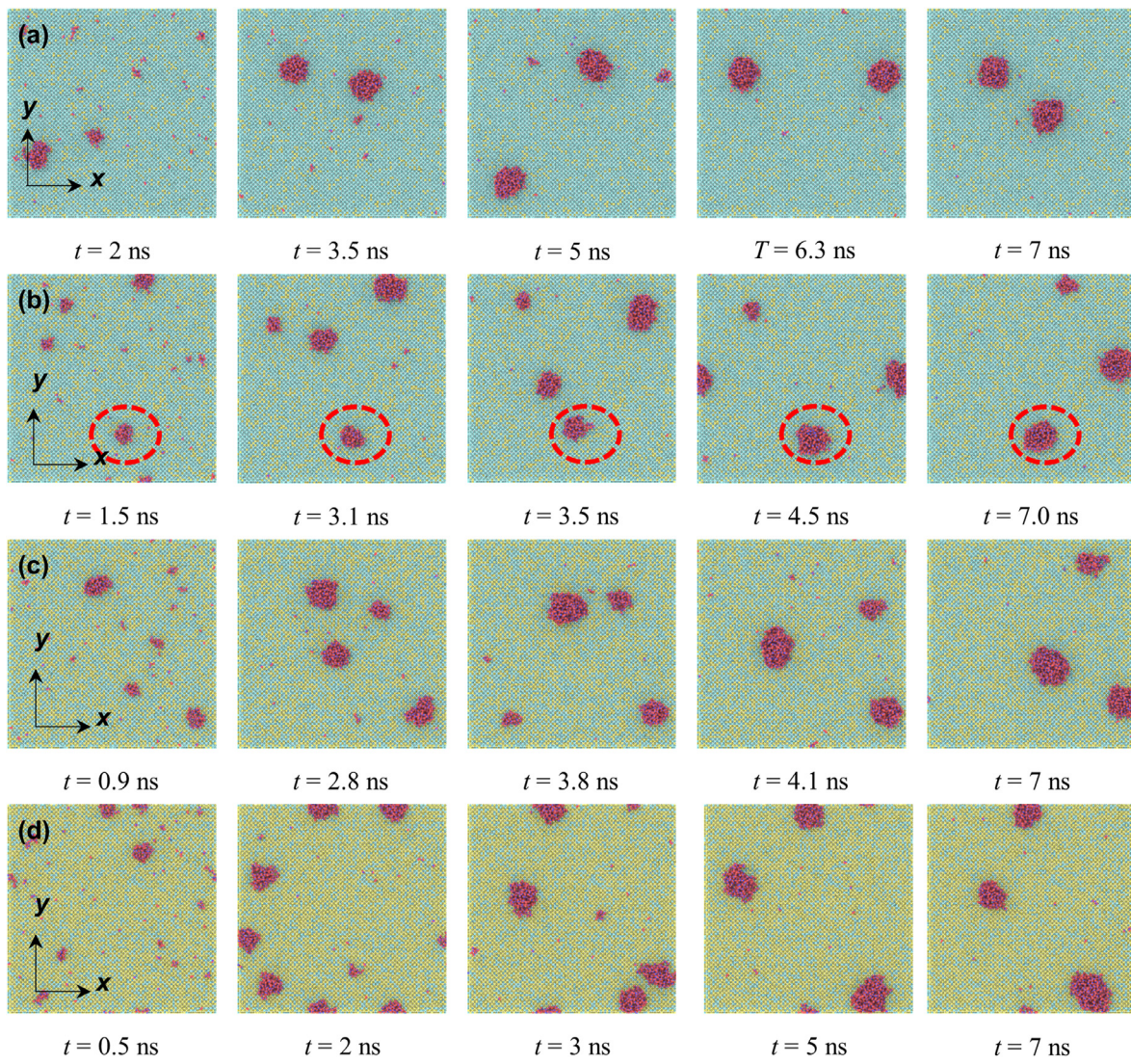


Fig. 9. Top view of the nucleation on binary mixed substrates with different hydrophilic atom ratio: (a) $r_m = 11.00\%$, (b) $r_m = 25.00\%$, (c) $r_m = 44.46\%$, and (d) $r_m = 69.44\%$.

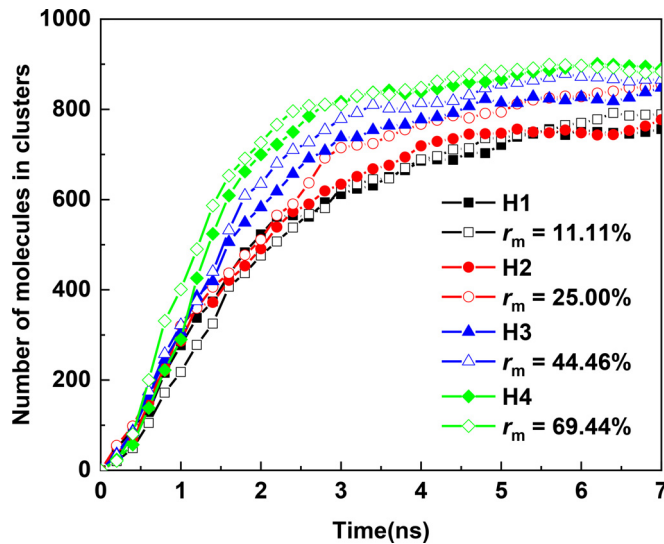


Fig. 10. Temporal evolutions for the number of condensed molecules in clusters for various substrates.

wettability (H1). The random nucleation processes observed indicate that the scattered hydrophilic atoms of a low hydrophilic ratio cannot distinctly increase the local energy of the surface, so no improvement on the nucleation rate is noted. For the substrate with a high ratio ($r_m = 69.44\%$), similar nucleation properties with the homogeneous substrate are yielded. Since the nucleation is dominated by high energy spots, the vapor needs to overcome the similar nucleation energy barrier for the two substrates of case group 4 to condense on the substrate surface, so the same nucleated water molecules are observed (Fig. 10). For case groups 2 and 3, the binary mixed substrates show enhancement of the nucleation rate because of the higher local energy difference. Thus, a moderate mixed ratio on the binary mixed substrate is considered to enhance nucleation performance. For the departure properties, the CAH of the binary mixed and the mono-wettability substrates are listed in Table 3. For the mono-wettability substrate, the CAH is increased with the solid-liquid interaction force. For the case groups listed in Table 3, the CAH on the binary mixed substrate and homogeneous substrate are close, indicating that the binary mixed substrate would not deteriorate the departure properties of the substrate surface. Combined the nucleation and departure properties, it can be deduced that a moderate hydrophilic atom ratio ($r_m = 25\%$) is needed to boost the condensation performance for the binary mixed substrates.

Noting that, the nucleation process is highly related to the local energy which depends on the interaction between the substrate and water molecules. Thus, the preferable hydrophilic atoms ratio would change with the different mixture pairs. Here, we perform another simulation of more hydrophilic atoms(38.1° for hydrophilic atoms and maintain 139.9° for hydrophobic atoms) with a ratio of 11.11%. The locations of the hydrophilic atoms are marked in red, as shown in Fig. 11(a). As expected, despite the decrease in mixed ratio, the increase of the hydrophilicity made the scattered hydrophilic atoms form potential nucleation sites(shown in Fig. 11(b)). The result indicates that the preferable hydrophilic atoms ratio will decrease when increasing the hydrophilicity of the hydrophilic atoms. And it also can be deduced that the ratio will increase when increasing the hydrophobia of the hydrophobic atoms.

Moreover, the Monte Carlo method is used to verify the above conclusion. Combine the distribution of the hydrophilic atoms with the surface potential energy analysis, the surface potential energy is highly related to the top layer of the substrate, as shown in

Fig. 12. Thus, to find the relationship of the distribution and the ratio of the hydrophilic atoms, only the surface(top layer) of the substrate is considered. Due to the vapor nucleation highly related to the local energy, the probability of one hydrophilic atom's neighborhood(cutoff radius of 8.16 Å) hydrophilic atoms number were calculated as schematic shown in Fig. 13(a). Theoretically, this probability obeys the hypergeometric distribution, but the binomial distribution remains a good approximation, and the probability of n hydrophilic atoms around a hydrophilic atom is:

$$P = C_{24}^n r_m^n (1 - r_m)^{24-n} \quad (n = 1, 2, \dots, 24) \quad (8)$$

where C is the binomial coefficient and r_m is the hydrophilic ratio. Meanwhile, the average frequency of one hydrophilic atom's neighborhood hydrophilic atoms number has been calculated with 1000 to 100,000 random times using the random generator mentioned in Section 2. As shown in Fig. 13(b), the frequency is consistent with the theoretical probability. Comparing the distribution of the hydrophilic atoms and the surface energy, a spot(radius of 8.16 Å) with 12 hydrophilic atoms can be rendered as a potential nucleation site. Thus, to find out the relationship between hydrophobic atoms ratio and the potential nucleation sites number, the Monte Carlo method(10,000 random substrates at one ratio) have been used to calculate the averaged quantity of spots with different number of nearby hydrophilic atoms. As shown in Fig. 14, until the hydrophilic ratio increase to 20%, the randomly distributed hydrophilic atoms can form some high energy spots. These enriched-hydrophilic spots can be rendered as nucleation sites despite the substrate without design.

In summary, combined the nucleation and departure properties, it can be deduced that a moderate hydrophilic atom ratio ($r_m = 25\%$) is needed to boost the condensation performance for the binary mixed substrates.

4. Conclusions

This study, via MD simulations, investigated the water vapor nucleation and water nanodroplet departure properties on the binary mixed substrate. A surface potential energy analysis was implemented to quantify the local energy of the substrate. A cluster analysis was performed to detail the nucleation processes on a binary mixed substrate. A body force was applied to the droplet to record the departure characteristics. The Monte Carlo method was used to obtain the regulation of the random distribution. Comparing with the homogeneous substrates with the same wettability, the binary mixed substrate shows enhancement on the vapor condensation. The main results of this work are listed as follows:

- (1) For the binary mixed substrate consisting of hydrophilic atoms and hydrophobic atoms, a linear relationship between the hydrophilic atom ratio r_m and the cosine value of the apparent contact angle was found. The apparent contact angle on the randomly mixed substrate could be estimated by the form of the Cassie equation.
- (2) The randomly distributed hydrophilic atoms of the binary mixed substrate could provide high local energy spots, and these spots are the active nucleation sites. The binary mixed substrate without special surface nano-texture design and manufacturing can effectively enhance the nucleation process.
- (3) The largest departure radius was used to characterize the droplet departure properties. The departure properties for the binary mixed substrate are the same as those for the contrast substrate.
- (4) Combined with the result of MD simulation and the Monte Carlo method, a low hydrophilic ratio cannot distinctly improve the condensation performance. For a high ratio ($r_m=69.44\%$ in this study), so the vapor molecules can overcome the nucleation energy barrier as the homogeneous substrate with same

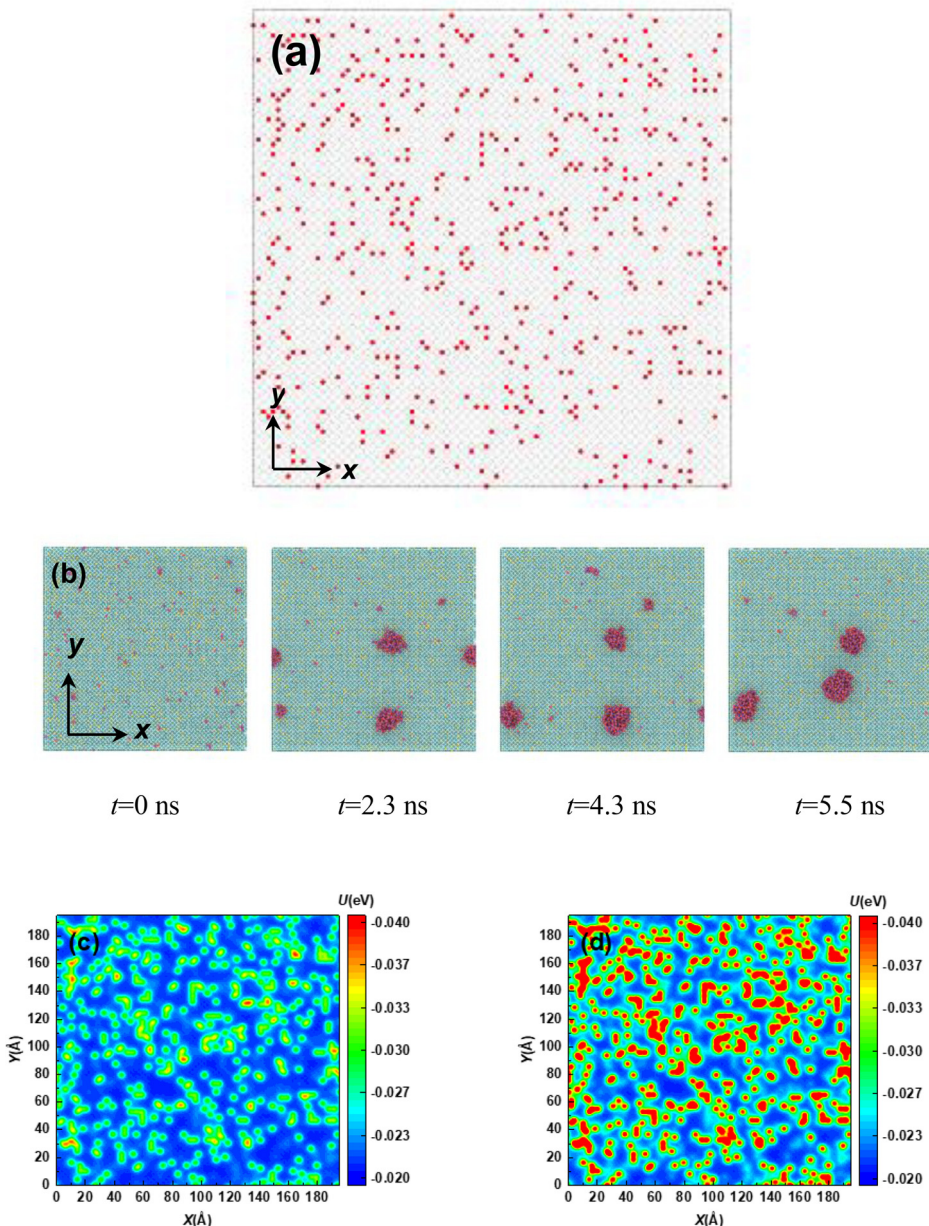


Fig. 11. (a) The distribution of the hydrophilic atoms (marked in red). (b) The snapshot of water vapor nucleation on binary mixed substrate ($r_m = 11.11\%$) with 38.1° for hydrophilic atoms and maintain 139.9° for hydrophobic atoms. Comparison between different mixture pairs of the surface potential energy: hydrophilic/hydrophobic atoms with the contact angle of (c) $74.9^\circ/139.9^\circ$, and (d) $38.1^\circ/139.9^\circ$

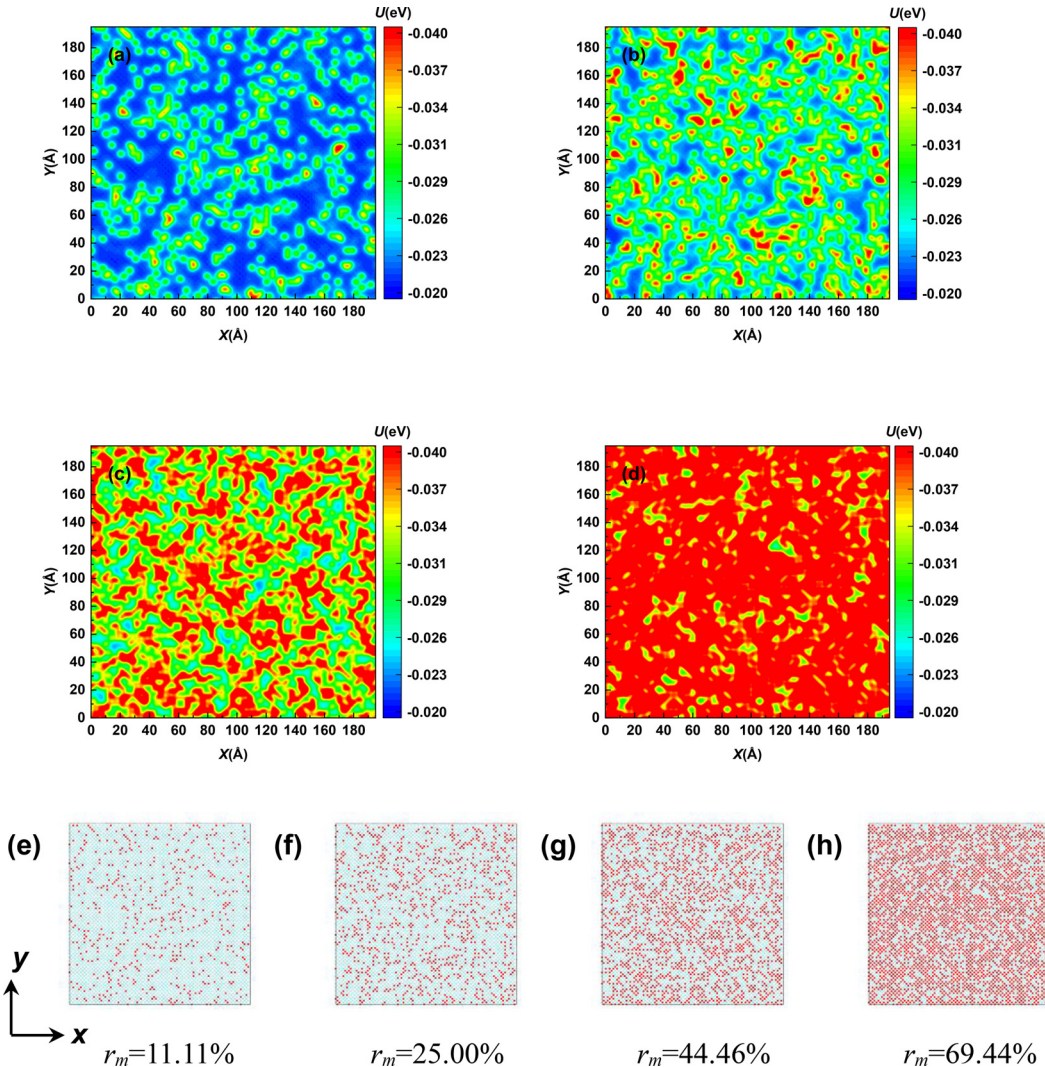


Fig. 12. The surface potential energy of binary mixed substrate: (a) 11.11%, (b) 25.00%, (c) 44.46% and (d) 69.44%. (e) to (h) is the snapshot of the substrate's top layer, and the hydrophilic atoms are marked in red. From this perspective, the surface potential is highly related to the distribution of the hydrophilic atoms of the substrate's first layer.

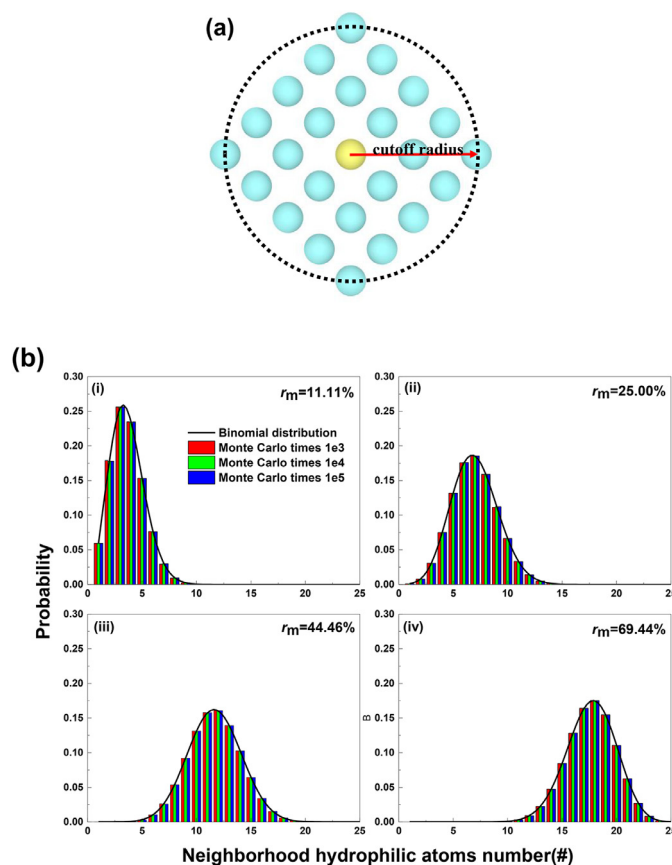


Fig. 13. (a) The schematic of the neighborhood(cutoff radius of 8.16 Å) atoms of a hydrophilic atom. (b) Two methods(theoretical and Monte Carlo method) to calculate the probability of one hydrophilic atom's neighborhood hydrophilic atoms number: the line is calculated by Eq. (8), and the column is the result of different random times(1000, 10,000, and 100,000) with different hydrophilic atoms ratio((i) 11.11%, (ii) 25.00%, (iii) 44.46% and (iv) 69.44%).

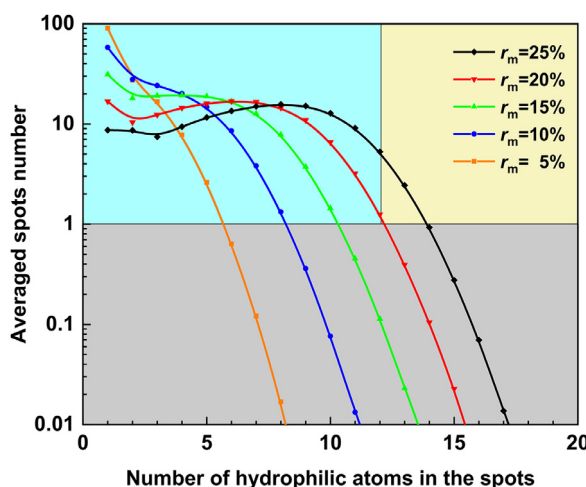


Fig. 14. The change of averaged spots number containing different number of hydrophilic atoms. When $r_m = 25\%$ and number of hydrophilic atoms in the spots is 12, the averaged spots number is 5.2: on an average of the binary mixed substrate with hydrophilic atom ratio is 25%, there are 5.2 spots with 12 hydrophilic atoms in this spots. With the judgment of whether there are 12 hydrophilic atoms in one spots, the left blue/right yellow area means a local low/high energy spot. The averaged spots number below 1 (marked in the gray area) means the spots with this number of hydrophilic atoms do not always occur.

wettability; conversely, the droplet departure would face difficulty. Thus, a moderated ratio ($r_m=25.00\%$ in this study) is considered in the binary mixed substrate as an ideal cooling surface with enhanced condensation performance.

Declaration of Competing Interest

The authors declare that they have no known competing financial interests or personal relationships that could have appeared to influence the work reported in this paper.

CRediT authorship contribution statement

Zi-Jie Wang: Conceptualization, Methodology, Investigation, Writing – original draft. **Shao-Yu Wang:** Data curation, Investigation, Software. **Dan-Qi Wang:** Investigation, Software. **Yan-Ru Yang:** Formal analysis, Resources. **Xiao-Dong Wang:** Funding acquisition, Project administration, Supervision, Writing – review & editing. **Duu-Jong Lee:** Supervision, Writing – review & editing.

Acknowledgments

This study was partially supported by the **National Natural Science Foundation of China** (No. 51936004), the Science Fund for Creative Research Groups of the **National Natural Science Foundation of China** (No. 51821004), and the **Fundamental Research Funds for the Central Universities** (No. 2020MS063).

References

- [1] S. Al-Kharabsheh, D.Y. Goswami, Analysis of an innovative water desalination system using low-grade solar heat, Desalination 156 (2003) 323–332.
- [2] B. Bhushan, Design of water harvesting towers and projections for water collection from fog and condensation, Philos. Trans. R. Soc. A 378 (2167) (2020) 20190440.
- [3] R.N. Leach, F. Stevens, S.C. Langford, J.T. Dickinson, Dropwise condensation: experiments and simulations of nucleation and growth of water drops in a cooling system, Langmuir 22 (21) (2006) 8864–8872.
- [4] P.J. Garcia-Nieto, Study of the evolution of aerosol emissions from coal-fired power plants due to coagulation, condensation, and gravitational settling and health impact, J. Environ. Manag. 79 (4) (2006) 372–382.
- [5] E. Schmidt, W. Schurig, W. Sellschopp, W. Versuche über die Kondensation von Wasserdampf in Film- und Tropfenform, Tech. Mech. Thermodyn. 1 (2) (1930) 53–63.
- [6] J.W. Rose, Dropwise condensation theory and experiment: a review, Proc. Inst. Mech. Eng. A 216 (2) (2002) 115–128.
- [7] N.A. Patankar, Mimicking the lotus effect: influence of double roughness structures and slender pillars, Langmuir 20 (19) (2004) 8209–8213.
- [8] C. Dorner, J. Rühe, Condensation and wetting transitions on microstructured ultrahydrophobic surfaces, Langmuir 23 (7) (2007) 3820–3824.
- [9] J.B. Boreyko, C.H. Chen, Self-propelled dropwise condensate on superhydrophobic surfaces, Phys. Rev. Lett. 103 (18) (2009) 184501.
- [10] N. Miljkovic, R. Enright, Y. Nam, K. Lopez, N. Dou, J. Sack, E.N. Wang, Jumping-droplet-enhanced condensation on scalable superhydrophobic nanostructured surfaces, Nano Lett. 13 (1) (2013) 179–187.
- [11] N. Miljkovic, R. Enright, E.N. Wang, Modeling and optimization of superhydrophobic condensation, J. Heat Transf. 135 (11) (2013) 111004.
- [12] A.R. Parker, C.R. Lawrence, Water capture by a desert beetle, Nature 414 (6859) (2001) 33–34.
- [13] K.K. Varanasi, M. Hsu, N. Bhave, W. Yang, T. Deng, Spatial control in the heterogeneous nucleation of water, Appl. Phys. Lett. 95 (9) (2009) 094101.
- [14] E. Ölceroglu, M. McCarthy, Self-organization of microscale condensate for delayed flooding of nanostructured superhydrophobic surfaces, ACS Appl. Mater. Interfaces 8 (8) (2016) 5729–5736.
- [15] B.L. Peng, X.H. Ma, Z. Lan, W. Xu, R.F. Wen, Experimental investigation on steam condensation heat transfer enhancement with vertically patterned hydrophobic-hydrophilic hybrid surfaces, Int. J. Heat Mass Trans. 83 (2015) 27–38.
- [16] T.S. Wong, S.H. Kang, S.K.Y. Tang, E.J. Smythe, B.D. Hatton, A. Grinthal, J. Aizenberg, Bioinspired self-repairing slippery surfaces with pressure-stable omniphobicity, Nature 477 (7365) (2011) 443–447.
- [17] K.C. Park, P. Kim, A. Grinthal, N. He, D. Fox, J.C. Weaver, J. Aizenberg, Condensation on slippery asymmetric bumps, Nature 531 (7592) (2016) 78–82.
- [18] S. Toxvaerd, Molecular-dynamics simulation of homogeneous nucleation in the vapor phase, J. Chem. Phys. 115 (19) (2001) 8913–8920.
- [19] S. Toxvaerd, Molecular dynamics simulation of heterogeneous nucleation at a structureless solid surface, J. Chem. Phys. 117 (22) (2002) 10303–10310.

- [20] T. Kimura, S. Maruyama, Molecular dynamics simulation of heterogeneous nucleation of a liquid droplet on a solid surface, *Microsc. Thermophys. Eng.* 6 (1) (2002) 3–13.
- [21] J.H. Pu, J. Sun, Q. Sheng, W. Wang, H.S. Wang, Dependences of formation and transition of the surface condensation mode on wettability and temperature difference, *Langmuir* 36 (1) (2019) 456–464.
- [22] S. Gao, Q.W. Liao, W. Liu, Z.C. Liu, Effects of solid fraction on droplet wetting and vapor condensation: a molecular dynamic simulation study, *Langmuir* 33 (43) (2017) 12379–12388.
- [23] W. Xu, Z. Lan, B.L. Peng, R.F. Wen, X.H. Ma, Effect of surface free energies on the heterogeneous nucleation of water droplet: a molecular dynamics simulation approach, *J. Chem. Phys.* 142 (5) (2015) 054701.
- [24] S. Gao, W. Liu, Z.C. Liu, Tuning nanostructured surfaces with hybrid wettability areas to enhance condensation, *Nanoscale* 11 (2) (2019) 459–466.
- [25] D.D. Xing, F.F. Wu, R. Wang, J. Zhu, X.F. Gao, Microdrop-assisted microdomain hydrophilicization of superhydrophobic surfaces for high-efficiency nucleation and self-removal of condensate microdrops, *ACS Appl. Mater. Interfaces* 11 (7) (2019) 7553–7558.
- [26] L.Q. Ai, H.S. Huang, Y.S. Zhou, M. Chen, Y.J. Lü, The oxidation of Fe/Ni alloy surface with supercritical water: a ReaxFF molecular dynamics simulation, *Appl. Surf. Sci.* 553 (2021) 149519.
- [27] S.Y. Wang, S.L. Wang, Y.R. Yang, X.D. Wang, D.J. Lee, High-temperature reactive wetting systems: role of lattice constant, *Chem. Eng. Sci.* 209 (2019) 115206.
- [28] M. Matsumoto, T. Nishimura, Mersenne twister: a 623-dimensionally equidistributed uniform pseudo-random number generator, *ACM Trans. Model. Comput. Simul.* 8 (1) (1998) 3–30.
- [29] S. Plimpton, Fast parallel algorithms for short-range molecular dynamics, *J. Comput. Phys.* 117 (1) (1995) 1–19.
- [30] S.M. Foiles, M.I. Baskes, M.S. Daw, Embedded-atom-method functions for the fcc metals Cu, Ag, Au, Ni, Pd, Pt, and their alloys, *Phys. Rev. B* 33 (12) (1986) 7983–7991.
- [31] P. Varilly, D. Chandler, Water evaporation: a transition path sampling study, *J. Phys. Chem. B* 117 (5) (2013) 1419–1428.
- [32] J.V.L. Beckers, C.P. Lowe, S.W. De Leeuw, An iterative PPPM method for simulating Coulombic systems on distributed memory parallel computers, *Mol. Simul.* 20 (6) (1998) 369–383.
- [33] W.C. Swope, H.C. Andersen, P.H. Berens, K.R. Wilson, A computer simulation method for the calculation of equilibrium constants for the formation of physical clusters of molecules: application to small water clusters, *J. Chem. Phys.* 76 (1) (1982) 637–649.
- [34] F.H. Stillinger, Rigorous basis of the frenkel-band theory of association equilibrium, *J. Chem. Phys.* 38 (7) (1963) 1486–1494.
- [35] A. Stukowski, Visualization and analysis of atomistic simulation data with OVITO—the open visualization tool, *Model. Simul. Mater. Sci. Eng.* 18 (1) (2009) 015012.
- [36] T. Young, III. An essay on the cohesion of fluids, *Philos. Trans. R. Soc. London* 95 (1805) 65–87.
- [37] M. Khalkhali, N. Kazemi, H. Zhang, Q.X. Liu, Wetting at the nanoscale: a molecular dynamics study, *J. Chem. Phys.* 146 (11) (2017) 114704.
- [38] A.B.D. Cassie, Contact angles, *Discuss. Faraday Soc.* 3 (1948) 11–16.
- [39] P. Bai, L.P. Zhou, X.Z. Du, Molecular dynamics simulation of the roles of roughness ratio and surface potential energy in explosive boiling, *J. Mol. Liq.* 335 (2021) 116169.
- [40] P. Dimitrakopoulos, J.J.L. Higdon, On the gravitational displacement of three-dimensional fluid droplets from inclined solid surfaces, *J. Fluid Mech.* 395 (1999) 181–209.
- [41] P.G. De Gennes, Wetting: statics and dynamics, *Rev. Mod. Phys.* 57 (3) (1985) 827–863.
- [42] S.D. Hong, M.Y. Ha, S. Balachandar, Static and dynamic contact angles of water droplet on a solid surface using molecular dynamics simulation, *J. Colloid Interface Sci.* 339 (1) (2009) 187–195.
- [43] F.C. Wang, Y.P. Zhao, Contact angle hysteresis at the nanoscale: a molecular dynamics simulation study, *Colloid Polym. Sci.* 291 (2) (2013) 307–315.